An Underactuated Gripper with Grasshopper-Inspired Linkages and Delay Triggering for Pinching and Adaptive Grasping*

Haokai Ding#, Yizhe Chen#, Dongjun Jia and Wenzeng Zhang, *Member, IEEE*

***Abstract*—Traditional parallel grippers require the adjustment of their position by a robotic arm when grasping objects on a table, which undoubtedly increases the difficulty of grasping planar objects of varying sizes. This challenge primarily arises from the circular trajectory exhibited by the fingertips during parallel grasping. To address this issue, this paper proposes a novel design for an adaptive gripper that combines both linear parallel grasping and adaptive grasping functions. Specifically, on the one hand, the characteristics of a locust linkage mechanism are utilized to achieve linear motion of the fingertips. On the other hand, a two-stage parallel four-bar linkage mechanism is applied to the gripper to ensure a fixed posture of the terminal finger segments. Additionally, an idle stroke transmission mechanism with delayed triggering is employed to achieve an adaptive grasping effect. Both theoretical and experimental results demonstrate that the proposed robotic hand exhibits excellent grasping performance and is suitable for industrial grasping applications.**

I. Introduction

The robotic hand is a crucial component of a robot, responsible for the fundamental function of grasping tools or objects to assist humans in accomplishing various complex tasks[1]. As machines find increasingly widespread applications across diverse fields, the functionality and performance of robotic hands continue to undergo continuous iterative upgrades.

Traditional robotic hands primarily originated from the need to clamp objects on industrial assembly lines. A typical example is the three-jaw chuck used on machine tools. These devices are capable of stably and firmly grasping workpieces, particularly those with symmetrical features, and are still widely employed in industrial settings to this day[2]. This grasping mode, which involves two or more fingers opening and closing towards each other, is known as the parallel grasping mode.

On the other hand, with the rapid development of humanoid robots, research on the hands of humanoid robots has also garnered significant attention[3]. Researchers have gradually developed various human-like hand grippers, namely multi-finger grippers or multi-finger robotic hands. Multi-finger robotic hands not only possess the ability to perform enveloping grasps by bending towards each other but can also achieve pinching actions at the fingertips. The former is suitable for power grasps, while the latter enables precise grasping, each with its own specific application domains. During the evolution of multi-finger hands, dexterous hands emerged. Dexterous hands are typically equipped with multiple fingers, each having more than two joints, and generally require nine actively driven degrees of freedom to achieve comprehensive manipulation capabilities.

Integrating more motors into robotic hands can enhance their dexterity but also leads to high costs. Especially as the number of motors increases, the control difficulty rises significantly. When grasping different objects in real-time, the demand for sensing and control becomes more demanding, which to some extent hinders the practical application and promotion of robotic hands[4]. In view of this, an intermediate approach that combines the practical low-cost advantages of industrial grippers with the diverse grasping modes of dexterous fingers has gradually emerged[5].

As early as several decades ago, some prosthetic hands designed for the disabled came into being[6]. These prosthetic hands not only mimic the appearance and basic grasping functions of human fingers but also utilize only a small amount of power from the human body such as chest expansion movements or a few motors for driving. This mechanism design approach, where the number of actuators is set to be fewer than the number of joints, is referred to as underactuation in the field of robotic hand design (it should be noted that this differs from the meaning of underactuation control in the control discipline).

In the past decade, underactuated finger technology has made significant progress. It has evolved from initially being able to only couple two or three joints to having forward or reverse coupling modes and later incorporating adaptive grasping modes to accommodate the grasping needs of objects with different shapes and sizes. Coupled grasping is a mechanism design approach that achieves multi-joint linkage through a single active degree of freedom, bringing numerous benefits to robotic fingers: it reduces design and control difficulties, enhances the enveloping grasping effect of the grasping mechanism, and makes the movements more anthropomorphic.

Reverse coupling is also a common coupling mechanism. It utilizes the opposite-direction linkage of two joints to keep the terminal finger segment always in a fixed posture relative to the base (i.e., the palm), thereby realizing the parallel grasping function. Parallel grasping, abbreviated as PG, refers to the terminal finger segment maintaining a constant posture

* Research supported by *Foundation of Open Research for Innovation Challenges (ORIC)*, X-Institute.

# These authors contributed equally to this work.

Haokai Ding is with Future Technology School, Shenzhen Technology University, Shenzhen, China and Laboratory of Robotics, X-Institute, Shenzhen, China.

Yizhe Chen, Dongjun Jia and Wenzeng Zhang are with Laboratory of Robotics, X-Institute, Shenzhen, China (corresponding author to provide email: zhangwenzeng@x-institute.edu.cn).

relative to the base from the initial state[7]. This grasping mode exhibits good versatility when grasping various objects on industrial assembly lines.

In addition, a type of adaptive grasping robotic finger, which is ingeniously designed by comprehensively utilizing transmission mechanisms, springs, and limit blocks, has also been invented one after another. During grasping, this finger can allow more than two finger segments to contact the object without prior knowledge of the object's shape and size. By driving only a single motor, it can achieve adaptive enveloping and grasping of objects with different shapes and sizes. Such fingers are called adaptive grasping robotic fingers. Fingers that combine the parallel grasping and adaptive grasping modes in a time-sequential manner are called parallel grasping adaptive robotic fingers, abbreviated as PG-adaptive fingers.

Currently, Robotiq, a Canadian company[8], has developed a PG-adaptive finger that can achieve both PG and adaptive grasping functions. However, during its PG grasping phase, although the terminal finger segment can realize the parallel grasping function, its motion trajectory is arc-shaped. This poses certain difficulties when grasping objects of different sizes on a table, such as the risk of colliding with the table surface where the object is placed. Therefore, it often requires the coordination and control of a robotic arm (on which the robotic hand is mounted at the end). This not only increases the control difficulty but also, during the deformation process of the PG object, in addition to the action of squeezing the object towards each other, the object is also moved in the height direction of the palm. This movement amount needs to be taken into account for precise grasping control, which are all shortcomings of this robotic hand.

To address this problem, this paper presents a novel design for an adaptive gripper, as shown in Fig. 1. This gripper integrates dual capabilities: linear parallel pinching and adaptive grasping. Specifically, on one hand, it leverages the characteristics of the Grasshopper-Inspired mechanism to achieve movement of the fingertip along a linear trajectory. On the other hand, a two-stage parallelogram linkage mechanism incorporated into the gripper ensures the distal phalanx maintains a fixed orientation.

Figure 1. Grasshopper-Inspired gripper developed in this paper.

II. Design of the Finger

A. Mechanism

The gripper comprises two symmetrically arranged, structurally identical fingers as shown in Fig.2 . Each finger incorporates the following components: a base, a motor, a worm gear, a worm wheel, a worm wheel shaft, a pinion gear, driver torsion pulleys, a driven torsion pulley, a torsion spring shaft, an output gear, an output driver gear, two phalanges, two joint shafts, a tension spring, and a limiting block.

The geared motor is fixed within the base. Its output shaft transmits power through the worm and worm wheel to the pinion gear. Left and right pinion gears mounted on the worm wheel shaft respectively drive the corresponding left and right driver torsion pulleys. These driver torsion pulleys actuate the single driven torsion pulley; the left driver pulley engages it via a left-hand torsion spring, while the right driver pulley engages it via a right-hand torsion spring. Consequently, the driven torsion pulley is driven by torsion springs of opposing handedness. Both the left-hand and right-hand torsion springs are pre-twisted to a specific angle, 60 degrees and installed under resistance between the three gears on the torsion spring shaft. This preload configuration effectively eliminates backlash during finger reversal, significantly accelerating the transition between grasping and releasing motions.

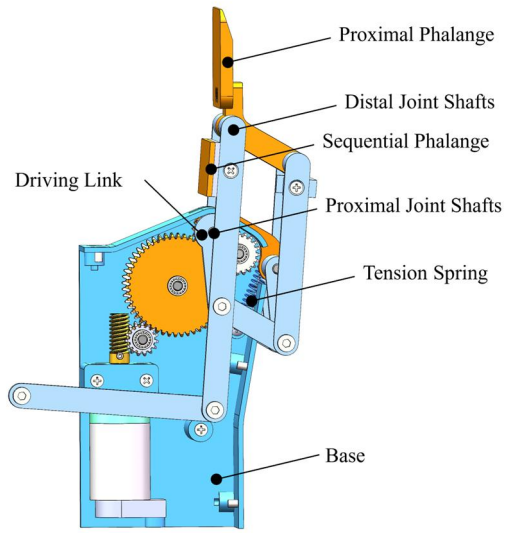

Figure 2. Grasshopper-Inspired Finger developed in this paper.

The driven torsion pulley meshes directly with the output gear, driving the output driver gear. This, in turn, rotates the proximal link of the driving mechanism. The mechanism employs a connecting rod assembly that constrains the distal phalanx to follow a linear trajectory. Furthermore, the integration of a two-stage parallelogram linkage ensures the distal phalanx maintains a fixed orientation relative to the gripper's base throughout its motion.

An idle transmission mechanism is positioned within the drive train downstream of a driver torsion pulley and prior to the output driver gear. It consists of a driver pulley incorporating a driver lug and a driven pulley incorporating a

driven lug. A designed angular clearance exists between these lugs, ensuring they remain unengaged in the initial state.

Upon motor actuation for grasping, the fingers initially execute a linear parallel pinching motion. This pinching phase ceases when the distal phalanx makes contact with an object.

B. Self-adaptation

Should the proximal phalanx encounter an object earlier than expected during the initial grasping approach, its subsequent motion is physically obstructed by the object's surface. This obstruction immediately generates a reaction force opposing the phalanx's intended trajectory. Consequently, the specific torsion spring associated with the obstructed side experiences a significant, measurable increase in torsional deformation beyond its preloaded state.

While the proximal phalanx remains constrained against the object, the geared motor continues to operate, transmitting undiminished torque through the drivetrain. This sustained input causes the driver pulley to rotate further, advancing its rigid driver lug angularly within the mechanism. This rotation continues until the advancing driver lug makes direct mechanical contact with the complementary driven lug on the driven pulley. Upon contact, the driver lug positively engages the driven lug, forcibly propelling the driven pulley into rotation. The rotation of this driven pulley directly modifies the configuration of the kinematically-coupled, two-stage parallelogram linkage system by altering the angular relationship of its constituent links. This deliberate change in the linkage geometry kinematically forces the distal phalanx to undergo a controlled relative rotation with respect to the now stationary proximal phalanx. The rotation of the distal phalanx continues only until its surface establishes firm contact with the object's profile.

This sequential contacting strategy – first the proximal phalanx is arrested, then the distal phalanx rotates into contact – constitutes the core mechanical process that dynamically enables the gripper's adaptive grasping functionality without preselecting contact points or requiring external sensors or complex control, leveraging only the intrinsic mechanical compliance and kinematic design.

III. Analysis of The Gripper

This section presents the kinematic analysis and grasping force evaluation for the finger mechanism. Utilizing the Complex Vector Method, we establish the finger's coordinate system to determine linkage angles and characterize the workspace. Model simplification involves neglecting gravitational forces acting on the finger components and frictional effects between phalanges. Contact forces are modeled as concentrated loads applied at discrete points.

A. Kinematic Analysis

For the Grass-hopper mechanism, we introduce vectors to analyze the closed-loop four-link mechanism. First, we place the mechanism in a Cartesian coordinate system. Take A as the starting point, the rod AD as a frame, coincides with the x-axis, and the parallelogram enclosed by each member is regarded as a closed vector polygon, and the direction of each vector is shown in the Fig. 5, and the direction angle of each vector and the x-axis is represented by $\Psi_1, \Psi_2, \Psi_3, \Psi_4$, where the constant angle Ψ_4 is equal to 0.

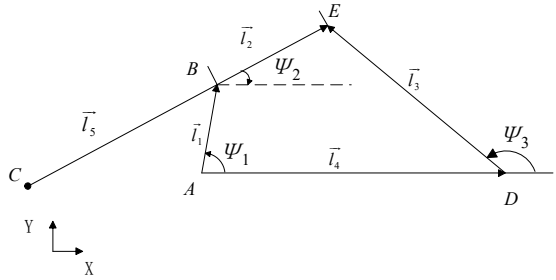

Figure 3. Closed quadrilateral vector diagram.

The functional elements comprise the distal phalange (DP), middle phalange (MP), and finger base (FB). A revolute joint connects the FB and DP, allowing the DP to achieve translational motion relative to the FB while maintaining independent rotational mobility.

It can be obtained from the projection of each vector on the x-axis and y-axis that

$$\vec{l}_1 + \vec{l}_2 = \vec{l}_3 + \vec{l}_4 \tag{1}$$

$$\begin{cases} l_1 \cos\Psi_1 + l_2 \cos\Psi_2 - l_3 \cos\Psi_3 - l_4 = 0 \\ l_1 \sin\Psi_1 + l_2 \sin\Psi_2 - l_3 \sin\Psi_3 = 0 \end{cases} \tag{2}$$

Eliminate the $\Psi_2$in the above equation to obtain:

$$E\cos\Psi_3 + F\sin\Psi_3 + G = 0 \tag{3}$$

where,

$$\begin{aligned} E &= l_4 - l_1\cos\Psi_1 \\ F &= -l_1\sin\Psi_1 \\ G &= \frac{E^2 + F^2 + l_3^2 - l_2^2}{2l_3}. \end{aligned} \tag{4}$$

Then, according to the triangular transformation formula, it can be obtained

$$\Psi_3 = 2\tan^{-1}\frac{F \pm \sqrt{E^2 + F^2 - G^2}}{E - G} \tag{5}$$

Because during the process of movement, Ψ_3 is always greater $\pi/2$, so

$$\Psi_3 = 2\tan^{-1}\frac{F - \sqrt{E^2 + F^2 - G^2}}{E - G} \tag{6}$$

Then it can be obtained by the above formula:

$$\Psi_2 = \tan^{-1}\frac{F + l_3\sin\Psi_3}{E + l_3\cos\Psi_3} \tag{7}$$

The rectangular coordinates of point C on the plane of link B are

$$\begin{aligned} x_C &= l_1\cos\Psi_1 + l_5\cos\Psi_2 \\ y_C &= l_1\sin\Psi_1 + l_5\sin\Psi_2 \end{aligned} \tag{8}$$

Then, the motion trajectory of the end point C could be counted through kinematic software. As Fig. 4. shows, point C moves in an approximate straight line within the range from 0.8 rad to 1.9 rad. And the chosen mechanism fails to close in the 2.10 to 4.16 rad. Finally, we use the least squares method to simulate a reasonable curve and calculate the vertical distance from each trajectory point to the line. If the root mean

square error (RMSE) and the maximum deviation value of the distance are below a preset threshold, it can be considered as an approximate straight line.

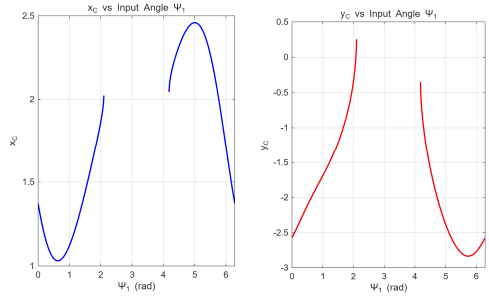

Figure 4. X and Y coordinates fitting and root mean square error analysis.

The instantaneous curvature of the trajectory point is calculated by taking discrete points, and if the curvature value is close to zero, it indicates that the trajectory has no obvious curvature. The RSME of X coordinate is 0.05 while the RSME of Y coordinate is 0.104. As shown in the Fig. 5, when the angle of Ψ_1 is in that interval, the trajectory of point C fits the straight line to the highest degree.

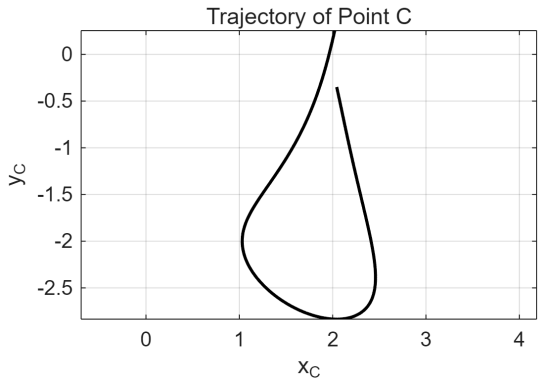

Figure 5. Motion trajectories of point C.

B. Grasping Force Analysis

In addition to the kinematic analysis, this section performs a static analysis, where a mechanical model is built on the base of the fingers, and the relevant physical symbols and their meanings are shown in the table.

Table I: Each physical symbols and theirs meaning

Valuables	Notation	Unit
F_1, F_2, F_3	Force of the 1st, 2nd and distal phalange	N
T	Torque transmitted by the desktop	N·mm
k_1, k_2	Coefficient of spring	N/mm
h_1, h_2, h_3	Vertical distance of the contact point of each phalange from the proximal joint.	mm

The parameters $\boldsymbol{T}_m$ is provided by the moment of the support force of the desktop to the distal phalange, and the relationship between the grasping force and the angle of the distal phalange can be obtained from the following equations, and when the angle increases, the grasping force of the terminal phalange increases.

$$\theta_0 + \theta_1 + \theta_2 = \pi + \Psi_2 \tag{9}$$

$$\boldsymbol{F}_2 = \left[F_2 \sin(\theta_0 - \Psi_2), -F_2 \cos(\theta_0 - \Psi_2)\right] \tag{10}$$

$$\boldsymbol{F}_3 = \left[F_3 \cos\theta_3, -F_3 \sin\theta_3\right] \tag{11}$$

$$\boldsymbol{G}_2 = \left(h_2 \cos(\theta_0 - \Psi_2), h_2 \sin(\theta_0 - \Psi_2)\right) \tag{12}$$

$$\boldsymbol{G}_3 = \left(l_5 \cos(\theta_0 - \Psi_2) + h_3 \sin\theta_3, l_5 \sin(\theta_0 - \Psi_2) + h_3 \cos\theta_3\right) \tag{13}$$

It can be obtained from the principle of virtual work:

$$\left[\boldsymbol{T}_m, -k(\theta_0 - \Psi_2)\right]\begin{pmatrix}\delta\Psi_2 \\ \delta\theta_3\end{pmatrix} = \left[\boldsymbol{F}_2\ \boldsymbol{F}_3\right]\begin{pmatrix}\delta\boldsymbol{G}_2^{\,t} \\ \delta\boldsymbol{G}_3^{\,t}\end{pmatrix} \tag{14}$$

$$\left[\boldsymbol{F}_2, \boldsymbol{F}_3\right]\begin{pmatrix}\delta G_2^{\,t} \\ \delta G_3^{\,t}\end{pmatrix} = \begin{pmatrix}h_2 & 0 \\ l_5\cos(\Psi_2 - \theta_0 + \theta_3) & h_3\end{pmatrix}\begin{pmatrix}\delta\Psi_2 \\ \delta\theta_3\end{pmatrix} \tag{15}$$

Thus, the grasping forces of the second and distal phalanges could be calculated.

$$F_2 = -\frac{k_1(\theta_0 - \Psi_2)}{h_3} \tag{16}$$

$$F_3 = \frac{\boldsymbol{T}_m}{h_2} + \frac{k_2\theta_3 l_5 \cos(\Psi_2 - \theta_0 + \theta_3)}{h_2 h_3} \tag{17}$$

Assuming k_1 = 180N/mm, k_2 = 0.12N/mm, h_2 = 30mm, h_3 =20mm and T_m =500N·mm. We can analyze the grasping forces of the second and distal phalange combined with the front equations, as shown in Fig.6.

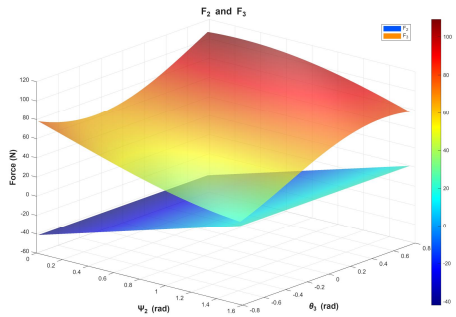

Figure 6. Grasping force of the second and distal phalange when the object is between the second and distal phalange.

When the finger enters adaptive mode and the object touches two of the three phalanges, Fig. 6 shows the forces on the object. Analysis is simplified by considering only the grasping forces from the second and last phalanges; analysis of the first and second phalanges yields the same result. The spring providing the limiting action applies force in the opposite direction.

IV. Experiments of the GI Finger

To thoroughly test the design's feasibility, we built a functional prototype. We carefully ensured kinematic compatibility and held manufacturing tolerances to ±0.15mm. Key structural parts—the housing, base, and anthropomorphic fingers—were 3D printed using fused deposition modeling on

a Bambu Lab A1 printer. We selected PLA (elastic modulus: 3.5GPa; tensile strength: 50MPa) as the material because it offers the best mix of performance and low cost, under $15 per unit. Print settings of 0.1mm layer height and 25% hexagonal infill achieved high dimensional accuracy at 98.7%.

As shown in Fig. 7, the GI finger successfully achieves Linear translation, demonstrating the functionality of the proposed design. The parallel grasping mode is realized through the precise alignment of the Grasshopper-Inspired Linkage (GIL) and the Double Parallelogram Mechanism (DPM), which maintain the orientation of the gripper during linear motion. This capability is critical for applications requiring high precision, such as pick-and-place operations in industrial automation or delicate object manipulation in medical robotics.

Figure 7. GI gripper and its linear parallel pinching of the GI gripper.

As shown in Fig. 8, the gripper demonstrates stable grasping capabilities for diverse objects. This versatility stems from the gripper's dual-mode operation, namely parallel grasping for symmetric objects and adaptive grasping for irregular shapes.

The parallel grasping mode ensures fingertip alignment along a straight line, while the adaptive mode allows the fingers to conform to the target object's contour, thereby enhancing grasping stability.

To evaluate the adaptive grasping performance of the GI gripper, we conducted experiments using an apple and a tape reel as test objects.

The results show that the middle phalange moves away from the object to adapt to its profile, while the distal phalange tilts toward the object to establish contact. This effectively demonstrates the adaptive grasping mechanism. This behavior relies on the passive compliance of the spring and the precise control of the driving link structure. Together, they enable the fingers to achieve dynamic reconfiguration based on the object's geometric shape.

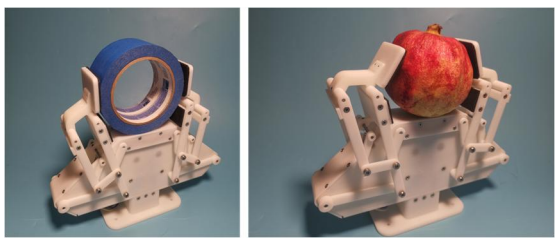

Figure 8. Two kind of grasping modes of the Grasshopper-Inspired gripper.

V. Conclusions

This paper presents a design scheme for a novel adaptive gripper. This gripper combines the compound functions of straight-line parallel grasping and adaptive grasping. On one hand, it utilizes the characteristics of a Grasshopper-like linkage mechanism to achieve linear motion of the fingertip trajectory. On the other hand, the application of a two-stage pantograph linkage mechanism to the gripper ensures the distal phalanx maintains a fixed orientation. Furthermore, an adaptive grasping effect is realized through the incorporation of an idle-stroke transmission mechanism triggered upon contact. Theoretical and experimental results both demonstrate the gripper's exceptional grasping capabilities.

This paper provides a detailed description of the GI finger mechanism and its operational modes. Mechanical and mathematical models are established to evaluate its performance. Finally, grasping capability experiments validate the design's feasibility and effectiveness, showcasing its potential in industrial and robotics applications.

References

[1] A. Billard and D. Kragic, “Trends and challenges in robot manipulation,” *Science*, vol. 364, no. 6446, p. eaat8414, Jun. 2019.

[2] T. Watanabe, K. Morino, Y. Asama, S. Nishitani, and R. Toshima, “Variable-Grasping-Mode Gripper With Different Finger Structures For Grasping Small-Sized Items,” *IEEE Robotics and Automation Letters*, vol. 6, no. 3, pp. 5673–5680, Jul. 2021.

[3] S. Kadalagere Sampath, N. Wang, H. Wu, and C. Yang, “Review on human-like robot manipulation using dexterous hands,” *Cognitive Computation and Systems*, vol. 5, no. 1, pp. 14–29, 2023.

[4] L. Kang, S.-H. Kim, and B.-J. Yi, “Modeling, Design, and Implementation of an Underactuated Gripper with Capability of Grasping Thin Objects,” *Machines*, vol. 9, no. 12, Art. no. 12, Dec. 2021.

[5] K. Feng, Z. Duan, C. Han, Z. Guo, and W. Zhang, “Underactuated Finger Topology for Humanoid Robot Grasp,” in *2024 International Conference on Advanced Robotics and Mechatronics (ICARM)*, Jul. 2024, pp. 753–758.

[6] S. Liu, W. Zhang, and J. Sun, “A coupled and indirectly self-adaptive under-actuated hand with double-linkage-slider mechanism,” *IR*, vol. 46, no. 5, pp. 660–671, Aug. 2019.

[7] H. Fu and W. Zhang, “A Novel Self-adaptive Robot Hand with Pin-array Structure Driven by Negative Pressure,” Aug. 2018.

[8] D. L.-A. Allen, S. Lefrançois, and J.-P. Jobin, “Gripper having a two degree of freedom underactuated mechanical finger for encompassing and pinch grasping,” US8973958B2, Mar. 10, 2015